Advanced Meteorological Information for Aviation - TH01010503

Tuning of 3D-Var ALADIN-CZ system for aircraft data assimilation.

Prague, July 19, 2016

Contents

List of Contributors:
Patrik Benáček *Czech Hydrometeorological Institute, Prague, Czech Republic*

In numerical weather prediction (NWP) an accurate high-resolution representation of the current state of the atmosphere is needed as an initial condition for the propagation of a weather forecast. Data assimilation provides techniques for combining observations of atmospheric variables with a model state of the atmosphere to obtain a consistent representation known as the analysis. The weighted importance of each contribution is determined by the size of its associated errors. Because of the magnitude (up to 10^6) and relatively unknown structure of these error correlations, the observation errors are assumed uncorrelated in most of the NWP centers. Although this assumption is reasonable for pairs of observations measured by distinct instruments, it is entirely inaccurate for the observations that are available at higher spatial frequency than the model resolution.

The assumption of zero correlations is often used in conjunction with spatial data thinning and/or the observation error inflation [8], [9]. Data thinning allows to reduce observation density so that spatial error correlations are not relevant. The error inflation is about increasing the observation error more than diagnostics suggest to eliminate other error correlations (e.g. inter-channel correlations) that are not reduced by data thinning. Guidance for selecting optimal thinning scales can be taken from [10] who found that thinning scales of a threshold observation error correlation value of around 0.2 produced the smallest analysis error when error correlations are neglected and the diagonal observation errors are not inflated.

Following the study [7], the Mode-S MRAR (MRAR) data assimilation in Aladin-CZ provides mostly neutral impact on the weather forecast. Following this study, we aim to tune the 3D-Var Aladin-CZ scheme in terms of data thinning, observation error setting and error inflation so that the a setting should provide better treatment of the MRAR into the analysis. The modifications are performed in three steps: we first study the horizontal and vertical error correlations to find an optimal distance for horizontal and vertical data thinning (in Sec 3). Secondly, we estimate the MRAR observation error based on the diagnostic method described by [11] (in Sec 4) and, finally, an optimal error inflation is estimated based on the forecast impact study (in Sec 5).

1 Data assimilation

1.1 3D-Var scheme

The operational use of the high resolution models requires assimilation techniques that should follow the issues such as numerical cost, robustness and the optimality of the solution. The best compromise is currently made by the 3D-Var (three Dimensional Variational) assimilation scheme [3]. This algorithm is based on Bayes' theorem deriving the analysis in terms of probability distribution functions. Provided that the observation errors ϵ_o and background errors ϵ_b are unbiased and mutually independent:

$$E[\epsilon_b] = E[\epsilon_o] = E[\epsilon_b(\epsilon_o)^T] = E[\epsilon_o(\epsilon_b)^T] = 0 \tag{1}$$

the analysis can be find by minimizing the quadratic cost function:

$$J(x) = \frac{1}{2}(x_b - x)^T B^{-1}(x_b - x) + \frac{1}{2}(y - h(x))^T R^{-1}(y - h(x)). \tag{2}$$

The cost function (2) measures the distance from the analysis state x to the observations y and the background state x_b, weighted by the inverse of their respective error covariances R and B. In order to compare observations with background, we use the observation operator $h()$ that allows to transform the model state space to observation space. The cost function minimization can be solved approximately to obtain the best linear unbiased estimate (BLUE), x_a [1]:

$$x_a = x_b + K(y - h(x_b))$$
$$K = BH^T(HBH^T + R)^{-1}$$

where H is the linearized observation operator given by $H = \frac{\partial h}{\partial x}|_{x_b}$. The 3D-Var algorithm seeks the minimum of (2) by performing several evaluations of the cost function and its gradient in order to approach the minimum using a suitable descent algorithm [3]. Although conceptually useful, 3D-Var treats observations as if they were valid at the same point in time, which is clearly an unrealistic assumption. In that case, the observation within a specific assimilation window although depending on time, are considered as observation of the analysis time. The length of assimilation window is usually set according to a type of observation.

1.2 Observation error

We have seen that the specification of the error covariances for both the background and observations will determine their weighted importance in the final analysis. The uncertainty associated with taking an observation sample is represented through an error vector ϵ_o. The error vector is assumed to have Gaussian distribution with zero mean and error covariance matrix $R = E[\epsilon_o(\epsilon_o)^T]$. The error covariance matrix R is comprised of the individual observation error variances on the diagonal and the error cross-covariances on the off-diagonals. A variance is defined as the mean-square deviation about the mean of the error data; a covariance is a measure of the association between two error variables.

Observation errors are distributed in the horizontal and vertical and can generally be attributed to four main sources: instrument noise, representativity error, pre-processing. In order to represent accurately the observations in a data assimilation system we must be able to correctly determine both the diagonal error variances and the off-diagonal cross-covariances. In order to study the off-diagonal elements of R directly, it can help to transform the error covariances into error correlations using the formula:

$$\rho_{ij} \equiv corr(\epsilon_i, \epsilon_j) = \frac{cov(\epsilon_i, \epsilon_j)}{\sqrt{var(\epsilon_i)var(\epsilon_j)}} \tag{3}$$

where ϵ_i and ϵ_j are the errors associated with an observation at point i and j in space, respectively.

In the current operational assimilation systems at the CHMI, all observation error correlations are assumed to be zero. This is a reasonable assumption for pairs of observations measured by distinct instruments. However under certain conditions this assumption is entirely inaccurate.

Observation error correlations can be vertically or horizontally distributed. If observations are used at a higher spatial frequency than the horizontal model resolution, then they will be affected by horizontal correlated errors of representativity because the model will be unable to represent the finer scale spatial structure given by the observations. Vertical errors of representativity will be present if the vertical model resolution is too low to represent a small scale physical feature as represented in the observation.

1.3 Observation error diagnostic

In order to simulate observation error correlations, we must have some understanding of the true error structure. This is not a straightforward problem because error covariances cannot be observed directly, only estimated in a statistical sense. Both the background, $y - h(x_b)$, and the analysis, $y - h(x_a)$, innovations are useful sources of information on the statistical properties of the errors. A method that address the separation of correlated observation and background errors was proposed by [11] (Desroziers method). The principle of this method is to use post-analysis diagnostics derived from linear estimation theory to statistically approximate the covariances of the observations, background and analysis errors in observation space. Using the assumption of mutually uncorrelated observation and background errors (1), we can find a statistical approximation of the observation error covariances:

$$E[d_a^o(d_b^o)^T] \approx R \tag{4}$$

where d_b^o and d_a^o are the background and analysis innovation vectors. The relation (4) should be satisfied provided the covariance matrices used in the cost function (2) are consistent with the true observation and background error covariances $E[\epsilon_o(\epsilon_o)^T]$ and $E[\epsilon_b(\epsilon_b)^T]$. This diagnostic can be used as a consistency check to ensure the observation error covariances are correctly specified in the analysis. For a simple case, Desroziers et al. (2005) show that the method has the capability of retrieving spatial correlation structures of observation errors, even if the initial assumed observation error is uncorrelated. This is possible as long as the true background errors and the true observation errors have sufficiently different correlation structures. Such results are encouraging because the diagnostic by its construction is nearly cost-free, and it allows the distinction between observation and background correlation structure. However, the relation (4) only holds exactly when the errors assumed in the assimilation are equal to those found in reality and the observation operator is linear. Care must therefore be taken when interpreting the results using these diagnostics.

2 Model Aladin-CZ

The limited area model ALADIN (Aire Limitee Adaptation Dynamique Developpement InterNational) is operated at the Czech Hydrometeorological Institute since 1994. We use a hydrostatic version that covers Middle Europe (2.1W-27.4E, 40.6N-55.7N) with horizontal resolution 4.7 km. The vertical resolution is fixed at 87 unequally spaced vertical levels covering the troposphere and then loosely the stratosphere up to 0.1 hPa. It is coupled every 3 hours with the ARPEGE forecast on its lateral boundaries.

The assimilation system at CHMI consists of a surface data assimilation (based on OI), the DF (Digital Filter) Blending [2] and 3D-Var assimilation scheme called together as BlendVar system [12]. This assimilation system uses a six-hour forward intermittent cycle, where the six-hour forecast from the previous cycle is used as a first guess. This guess is enhanced by surface data assimilation which updates surface parameters in a surface model scheme. In upper-air the long scales are blended with the global analysis from ARPEGE using DF Blending [2] as the global model is able to capture the long-scale synoptic waves more accurately than the limited area model. This background field is subsequently improved by observations in the upper-air data assimilation scheme which provides the best initial conditions for the following 6h-forecast. The BlendVar scheme is performed at 00, 06, 12 and 18 UTC.

The Mode-S MRAR involve around 140.000 per day (66% above 6000 meters) and a typical reporting frequency is 10 s. This observations are collected in the current assimilation scheme within ± 1.5 hour (3h-assimilation window) around the analysis time.The MRAR observations used actively in data assimilation are pre-selected by the white list described more in details in [7]. This white list was prepared during the period July till October 2015 and includes a list of 203 aircrafts with reliable observations. Currently, there is used 50 km horizontal thinning and no vertical thinning for aircraft observations in the Aladin-CZ model. The vertical profile of observation errors for AMDAR data is applied also for MRAR supposing that both aircraft types have similar platforms. The quality and distribution of the AMDAR and MRAR observations is described in [7].

3 Diagnostic of spatial error correlations

Data

The spatial error correlations are estimated for MRAR observations based on Eq. 4 and Eq. 3. All possible d_b^o and d_a^o pairs are binned by separation distance using a binning interval of 10 km (horizontal) and 4 hPa (vertical). The observations in each pair are less than 1 hour apart from background or analysis. The horizontal error correlations are diagnosed at specific pressure levels (± 2 hPa) that correspond approximately to aircraft flight levels between $150 - 300$ hPa (see Fig 1). The vertical error correlations are diagnosed based on the pairs collected between $400 - 950$ hPa where the ascending/descending legs of the flights provide a suitable observation sample.
The background/analysis departures were taken from the 3D-Var assimilation system, using only data that were actively assimilated and pass the quality control checks. For this diagnostic purpose, the Mode-S data are assimilated with 5-km horizontal thinning to get the 5-km minimum separation distance. The diagnostics are evaluated for a summer (05 Jul - 30 Jul 2015) and a winter period (25 Feb - 25 Mar 2016) to include some seasonal variations in the statistics.

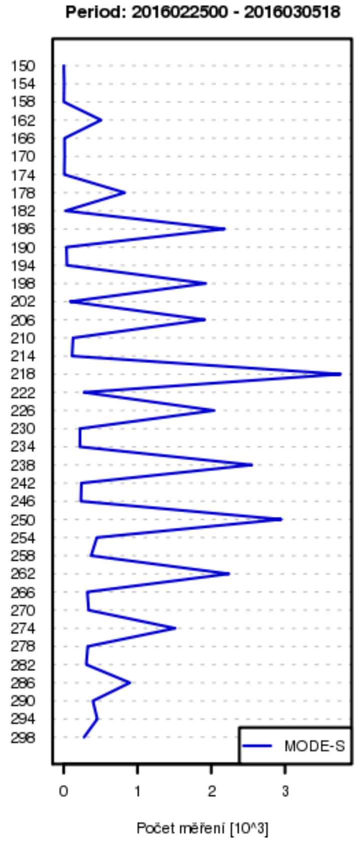

Figure 1: The observation number of MODE-S for pressure levels between 400-150 hPa.

Results

The horizontal observation error correlations as a function of separation distance are examined for the selected pressure levels 187 ± 2 hPa, 216 ± 2 hPa, 264 ± 2 hPa, 276 ± 2 hPa, 300 ± 2 hPa and 392 ± 2 hPa in Fig 2. Firstly, note that a number of observation pairs decreases with the separation distance more significantly below the pressure level ~ 250 hPa (compare the top and bottom Fig 2) where the flight levels are replaced by ascending/descending legs of the flight. Secondly, the horizontal error correlations increase below the separation distance $25 - 35$ km detected for the levels between $150 - 250$ hPa. The higher error correlations are also detected between $300 - 400$ hPa, however, this error correlation increase is probably affected by the less observation sample in these levels. In the lower-troposphere,the horizontal error correlations are neglected due to ascending/descending legs of a flight. Following the paper [10], the optimal analysis corresponds to the error correlations that are less than 0.2 for temperature variable. It corresponds to the MRAR horizontal data thinning between $25 - 35$ km.

The vertical observation error correlations as a function of altitude distance are shown in Fig 3. The vertical error correlations are for temperature around 0.2 and this value increases since the separation distance is less than 18 hPa. Than we estimate the optimal vertical thinning distance between $15 - 20$ hPa.

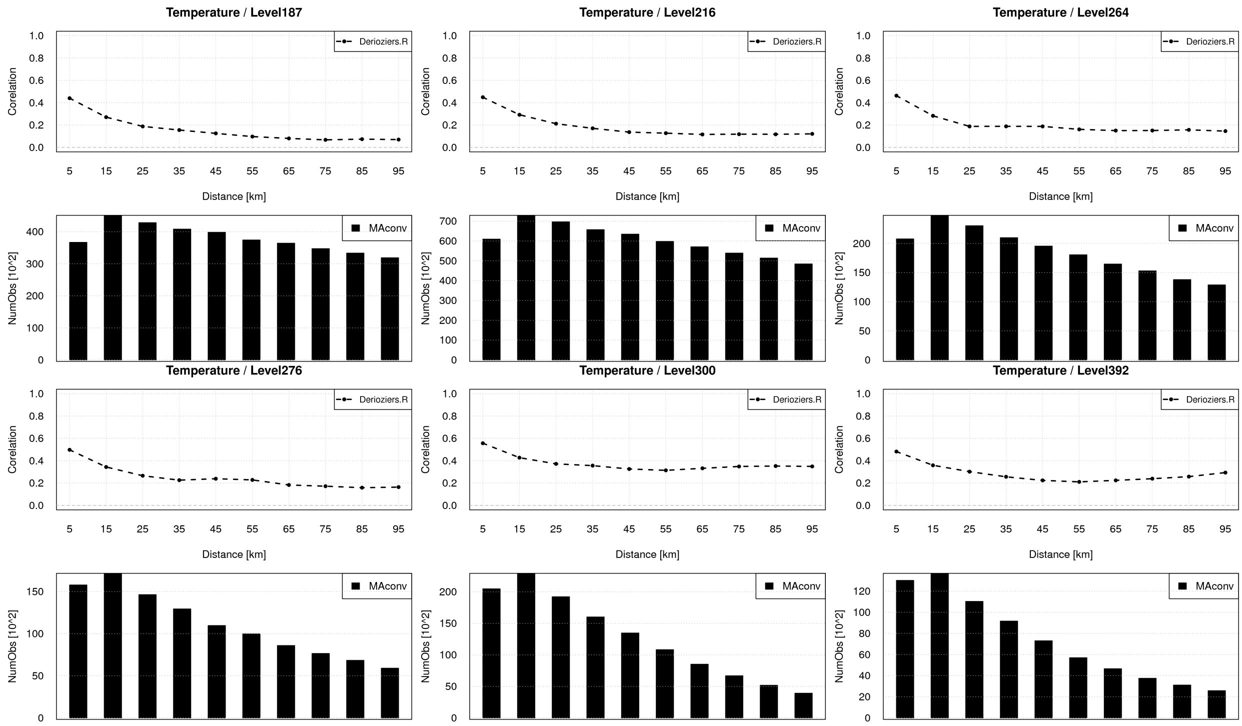

Figure 2: Estimates of horizontal observation error correlations based on Desroziers diagnostic (top) and the number of a collocations (bottom) as a function of separation distance for MODES-S observations.

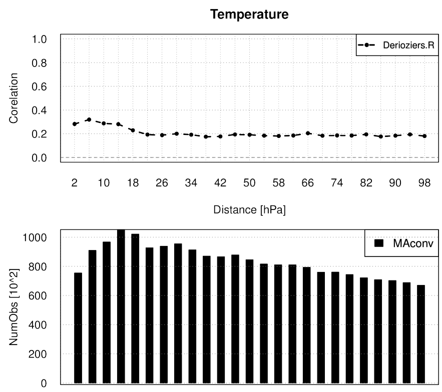

Figure 3: Estimates of vertical observation error correlations based on Desroziers diagnostic (top) and the number of a collocations (bottom) as a function of separation distance for MODES-S observations.

3.1 Spatial data thinning

Following the results of the spatial observation error correlation in Sec 1.3 we investigated the impact of the both horizontal and vertical thinning of MRAR data on the weather forecast. Technical details of setting of the data thinning in 3D-VAR Aladin system are described in Appendix A. At the moment the same thinning distance is applied for both MRAR and AMDAR observations since these types have not been distinguished (technically) in the current assimilation system yet. Consequently, we examine the mixed forecast impact of MRAR and AMDAR observations (called aircraft observations). The observation number reduction using horizontal and vertical thinning is shown for AMDAR and MRAR observation in Fig 4. Note that the higher data reduction is detected for MRAR than AMDAR observations. While the horizontal thinning reduces the aircraft observations between $200 - 700$ hPa (the left Fig 4), the vertical thinning reduces the observations between $500 - 850$ hPa (the right Fig 4).

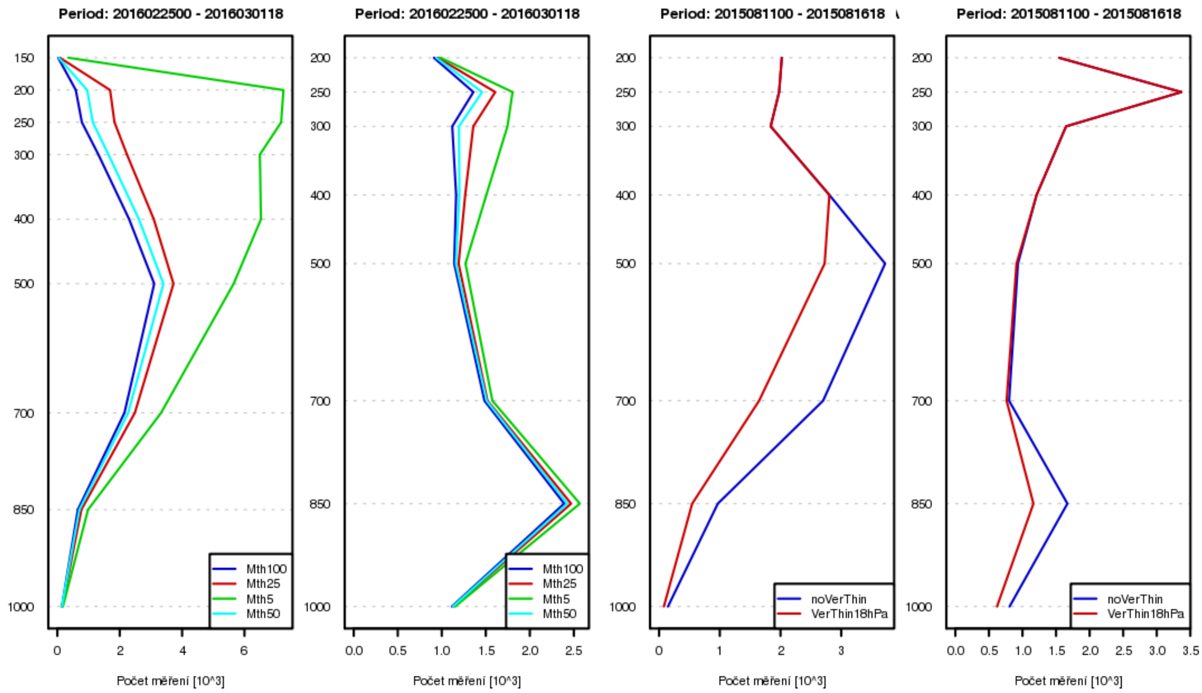

Figure 4: Reduction of aircraft observations using horizontal and vertical thinning. From left: horizontal thinning for MRAR, AMDAR and vertical thinning for MRAR, AMDAR. The data are collected at all analysis times for 6 days period.

Horizontal thinning

The impact of horizontal thinning on analysis and subsequent forecast is examined for the period 25 Feb - 05 Mar 2016. We thin the aircraft data to an approximately distance 5 km (MAosTh5), 25 km (MAosTh25), 50 km (MAosTh50) and 100 km (MAosTh100). In Fig 5 is shown the impact of the thinning distance setting on RMSE of analysis (top) and 3-h forecast (bottom) with respect to MRAR observation. In analysis, we detected a positive impact of 5-km data thinning since the analysis is verified against MRAR data. On the other hand, the negative impact on analysis is detected since we verify against TEMP observation (not shown). This affirms the hypothesis that the aircraft data could improve analysis locally, however, the signal propagation through isotropic and homogeneous B-matrix could worse the quality of analysis outside the observation points [5]. Consequently, the analysis impact is irrelevant in terms of analysis quality and the relevant information could provide a short-term forecast, at which observation increments are well balanced (after 3-hours spin up) with the model state. The 3-h forecast impact of horizontal thinning is shown in the bottom Fig 5. The negative impact of the 5-km thinning is detected in the upper-troposphere (200 – 300 hPa), while slight positive impact on the temperature and wind speed forecast (RMSE) is detected for the 25-km thinning. These results are in agreement with the study of the spatial observation error correlations in Sec 3, where the 25 – 35 km thinning distance was estimated as low-threshold provided an optimal analysis.

Vertical thinning

The forecast impact of vertical thinning is examined for the period 11 Aug - 16 Aug 2015. We thin the aircraft data to an approximately distance of either 15 hPa or 5% pressure difference, whichever is smallest (see the left Fig 4). It allows to reduce the use of excessive ascend/descend measurements near airports. The positive effect of vertical thinning is detected for the 3-h forecast of the wind speed

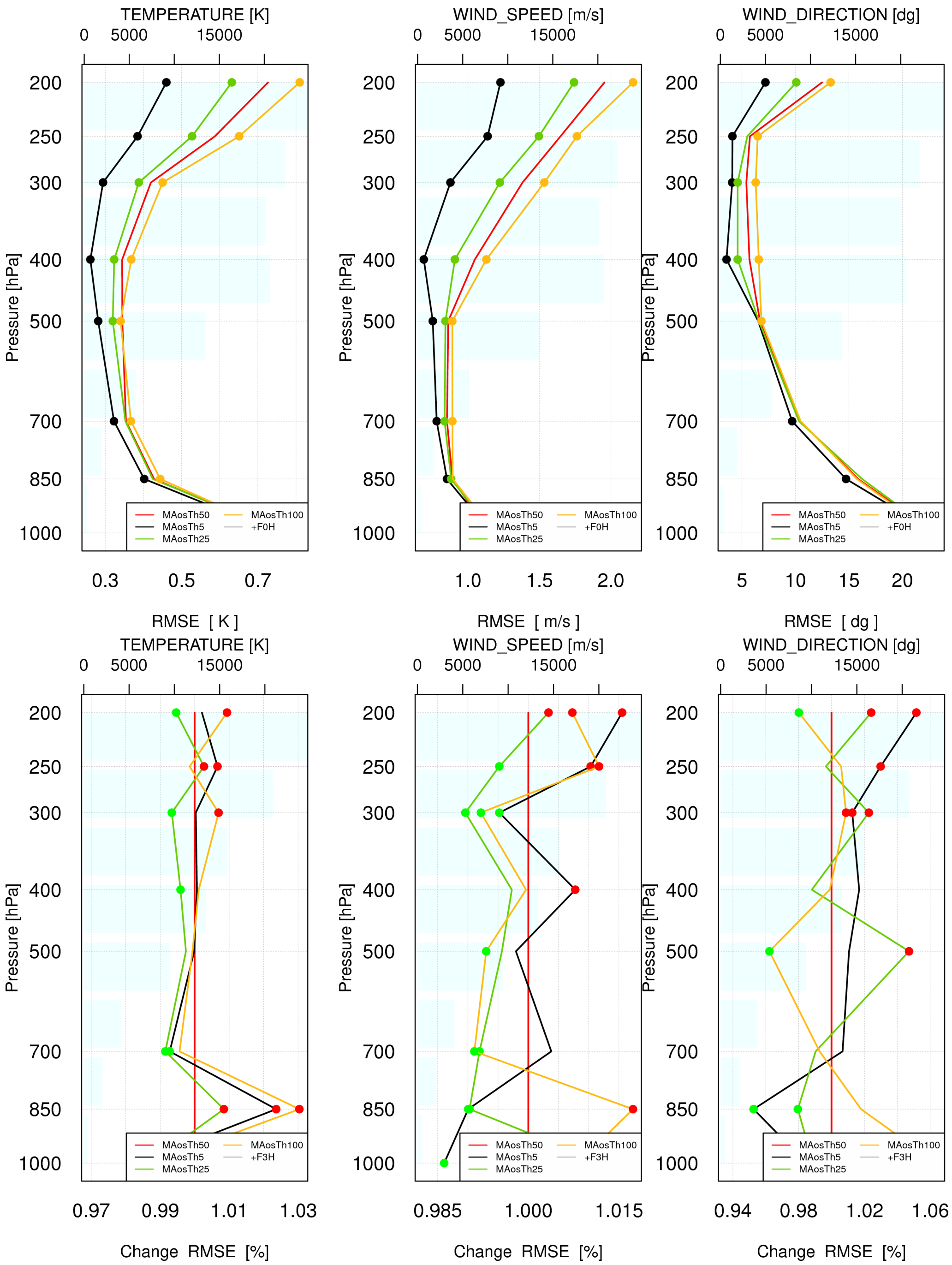

Figure 5: The RMSE impact of 5-km (black), 25-km (green), 50-km (red) and 100-km (yellow) thinning distance on analysis (top) and the 3-h forecast (bottom) with respect to MRAR.

and wind direction profile (see Fig 6). In terms of the long-term $3-6$ h forecast, we detect a positive impact on the RMSE of wind speed between $500-1000$ hPa verified with respect to MRAR (Fig 7) and TEMP (not shown) observations.

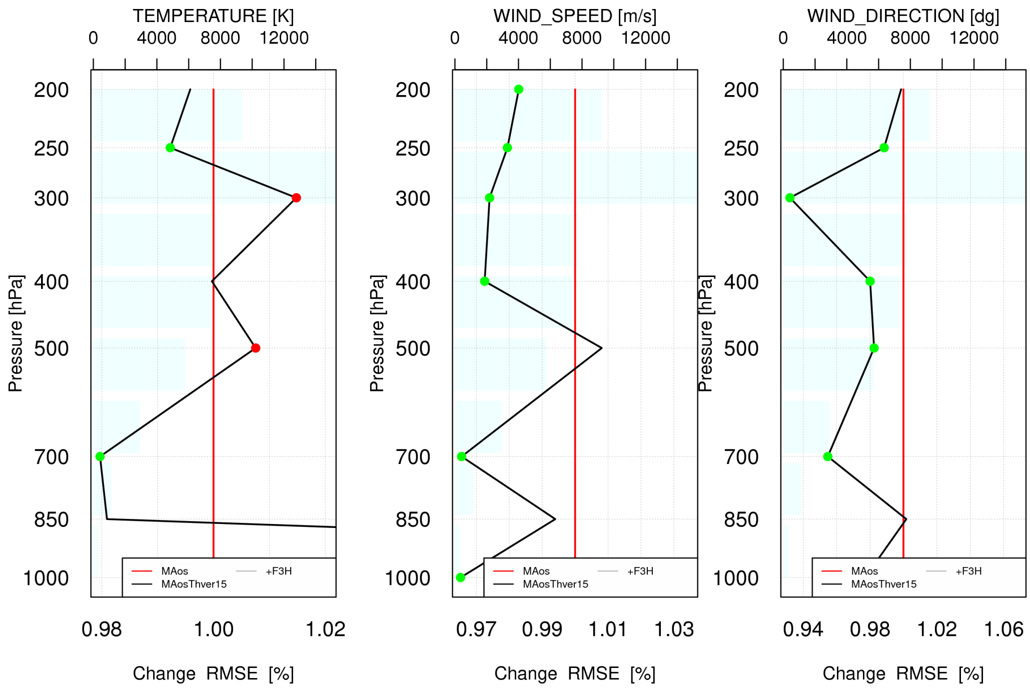

Figure 6: The impact of vertical thinning on the relative change of RMSE for 3-h forecast. The scores are computed with respect to MRAR observation.

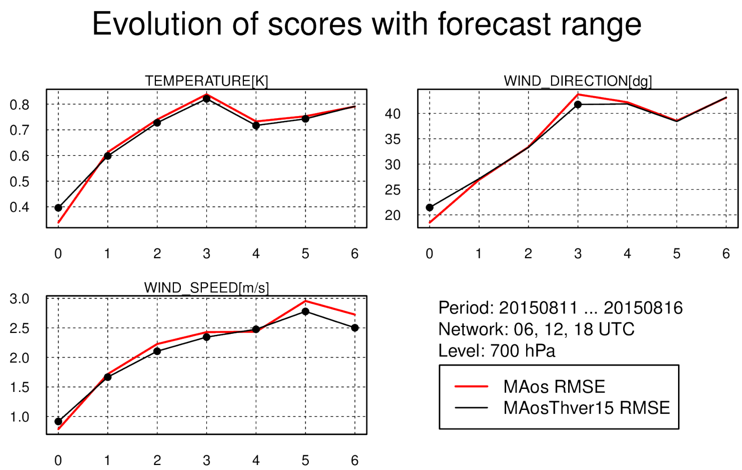

Figure 7: The impact of vertical thinning up to 6h forecast ranges for the pressure level 700 hPa. The scores are computed with respect to MRAR observation.

4 Diagnostic of observation error

The observation errors included in diagonal **R** are estimated by Desroziers method [11] for the AMDAR and MRAR observations. The scores are evaluated for the three months period 01 Jul - 30 Sep 2015.

The observation error estimations are shown in Fig 8. Note that the errors estimated by the Desroziers (solid line) are similar between the both aircraft types. Slight differences are detected for the temperature profile and for wind components below 850 hPa. The latter difference of the estimated error could be explained by less MRAR observation number (below 850 hPa) so that the convergence of the error estimation is slower (for more detail see Appendix B). Whereas in the higher-troposphere, the error-estimations are over-estimated probably due to the violation of the Desroziers method assumptions (1) namely the independence between observation and background error. The observation errors assumed in the 3D-Var Aladin-CZ (dotted line) have similar shape as the Desroziers error, but about 30% overestimated.

As a result, the same observation error setting might be used for the both AMDAR and MRAR observations. Furthermore, it would be desirable to use more iterations in the Desroziers method to improve the observation error estimation in the higher-troposphere and near the surface (for more details see Appendix B).

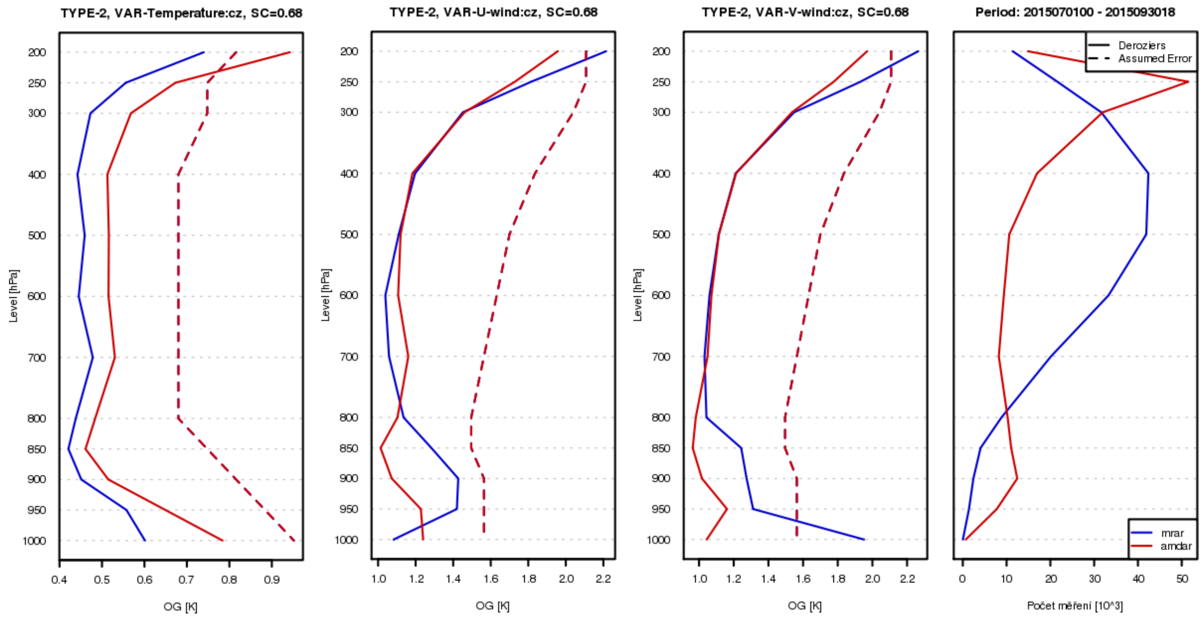

Figure 8: Observation error estimations for the AMDAR (red) and MRAR (blue) measurements based on Desroziers method (solid) and the observation error assumed in the 3D-Var Aladin-CZ system (dotted). In addition the systematic errors (dashed) are detected. The scores are computed for the CZ domain.

In addition, the bias values (mean of d_b^o) for AMDAR and MRAR observations are shown in Fig 8 (dashed line). There is a similar bias between the both aircrafts for the both wind-components and a slight increase is detected for the MRAR data for temperature in the lower-troposphere. The investigation of the bias value between Prague and Vienna airports provides high variations in vertical profiles (not shown). This error variations are probably caused by a different conditions near surface such as vegetation and orography or the biases could also depend on aircraft types [4].

4.1 Observation error inflation

An optimal observation error inflation is examined for the AMDAR and MRAR observations with regards to a forecast quality. The error inflation is handled by sigma coefficient through screening namelist that represents a multiplication factor to observation error setting in the assimilation scheme. The sigma coefficient is increased from ~ 0.7 (default sigma setting in the 3D-VAR Aladin-CZ) to 5 by the step 0.7. The sigma coefficient is changed for the both AMDAR and MRAR observations supposing that their observation error is similar (see Fig 8). The forecast quality is evaluated for various sigma setting of the AMDAR/MRAR observations. This study is based on assimilation experiments performed during 10-days period (25 Feb - 5 Mar 2016).

The forecast impact of the various sigma coefficients is evaluated with respect to AMDAR observations. In Fig 9, there are the overall RMSE scores for the 3-6h forecasts and all vertical levels between $150-950$ hPa for temperature (T), wind speed (WS) and wind direction (WD). The minimum forecast error (minimum RMSE score) is detected for the sigma coefficient around 2. Note that the current

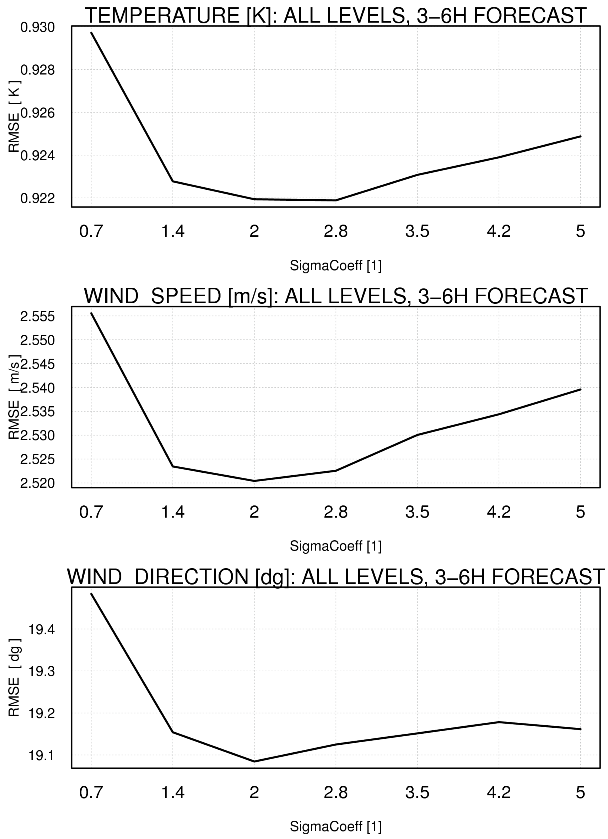

Figure 9: The RMSE scores for the 3-6h forecast and all levels between $150 - 950$ hPa with regards to various sigma coefficients. The scores are evaluated against AMDAR observations.

sigma setting in Aladin-CZ (~ 0.7) provides the degradation of forecast. Similar results are detected when we verify against MRAR and TEMP observations (not shown).

5 The tuned assimilation scheme: Forecast impact study

Following the results in the sections 3.1 and 4.1, we modify the spatial data thinning and observation error inflation for MRAR and AMDAR in the 3D-VAR Aladin-CZ system. The forecast impact is examined for 20-days period 25 Feb - 15 Mar 2016. We run the 6 hour assimilation cycle with +48 hours forecast production run at analysis times 6 and 12 UTC. The experimental settings are described in the following table. The forecast impact is evaluated with regards to TEMP, AMDAR and MRAR observations. We use two verification domains over LACE (computational domain Aladin-CZ) and over an extended CZ domain (ext-CZ). The ext-CZ domain is set with regards to the coverage of MRAR observations [7]. This ext-CZ domain is well-covered by AMDAR and MRAR at the upper levels, whereas there are limited TEMP observations available at 00, 12 UTC (12 stations) and even less at 06 and 18 UTC (5 stations).

Experiment	**Assimilated data**	**Horizontal thin**	**Vertical thin**	**Inflation factor**
MAconv	conv, amdar, mrar	50 km	no	~ 0.7
MAconv_new	conv, amdar, mrar	25 km	15 hPa	2
Aconv_new	conv, amdar	25 km	15 hPa	2

The forecast impact of the tuned 3D-VAR system is assessed comparing MAconv and MAconv_new experiments over the LACE domain. The RMSE (top) and MAE (bottom) scores are evaluated with respect to TEMP in Fig 10. We detect a significant positive impact of the tuned system (MAconv_new) on the relative humidity (RH), T, WS and WD forecast up to 1-2 days for the whole vertical profile. This positive impact is detected for T and WS mostly in the upper-troposphere (between 200-300 hPa), whereas the short-range forecast improvement (up to 12 hours) is detected in the middle- and lower-troposphere.

The impact of MRAR data for the tuned system is assessed comparing Aconv_new and MAconv_new experiments over the ext-CZ domain. The RMSE (top) and MAE (bottom) forecast impact of MRAR is evaluated with respect to TEMP (see Fig 11) and AMDAR (see Fig 12) observations. The both verifications have common the positive impact on WS and WD forecast up to 36 hours (between $300 - 400$ hPa). On the other hand, the differences between the AMDAR and TEMP verifications are detected for T and WS in upper- (250-400 hPa) and lower-troposphere (700-850 hPa). In the low-troposphere, the positive impact on T and WS up to 12 hours is detected only against AMDAR (not against TEMP). This could be explain by the location of aircraft data around airports in the lower-troposphere since there dominate the ascending/descending legs of flights. In the upper troposphere, we detected positive impact on T up to 12 hours against AMDAR (see Fig 12), however, there is negative impact on T against TEMP (see Fig 11). This inconsistency could be explain by a warm bias in TEMP data caused by the radiosonde balloon drift in upper levels [6] that is not considered in the Aladin-CZ verification.

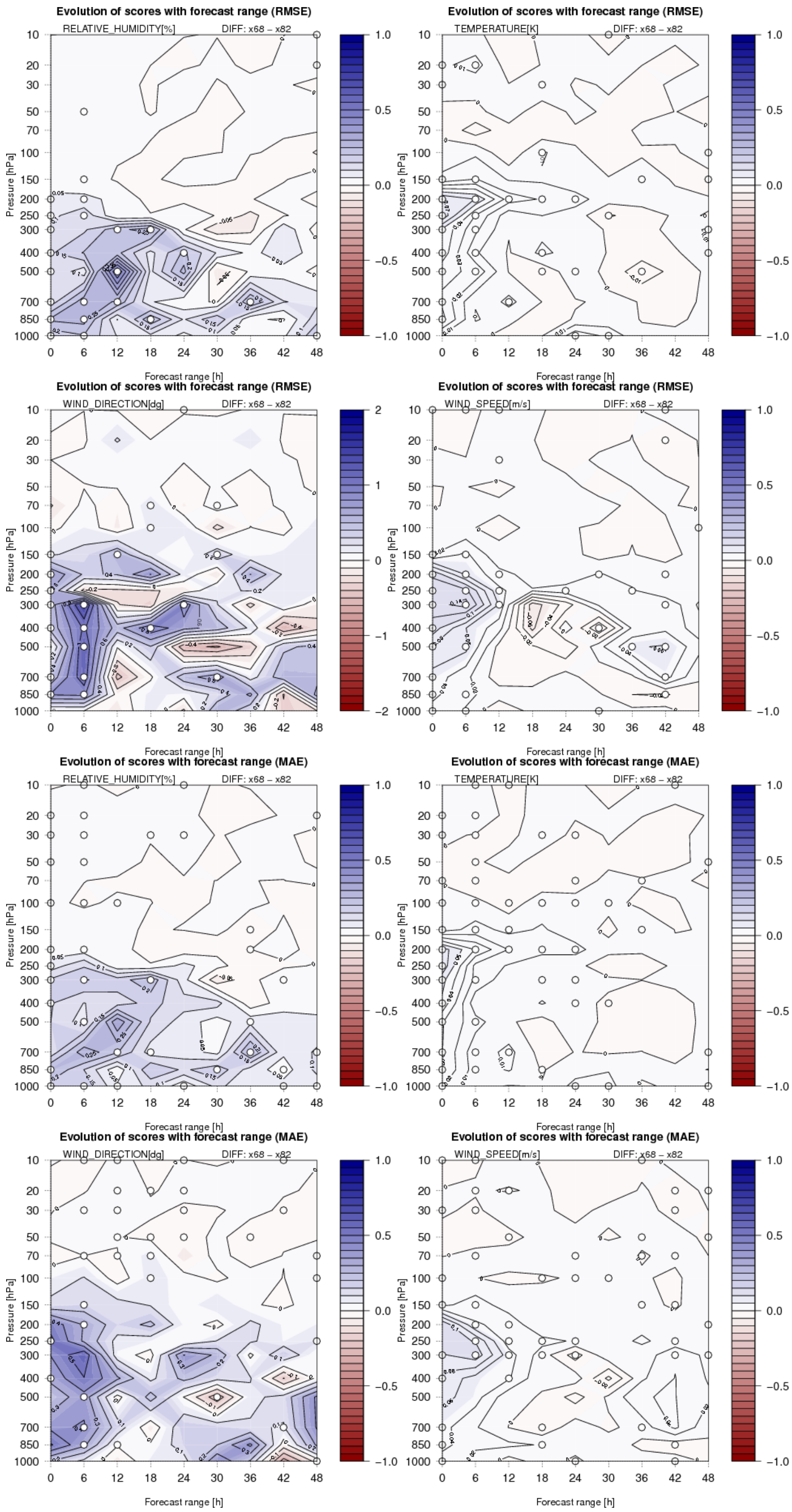

Figure 10: The forecast impact of AMDAR and MRAR data assimilation before and after a tuning the 3D-VAR assimilation system. The RMSE (top) and MAE (bottom) scores are evaluated with regards to TEMP observation. The improvement/degradation is represented by blue/red color. The white points represents 95% significance level.

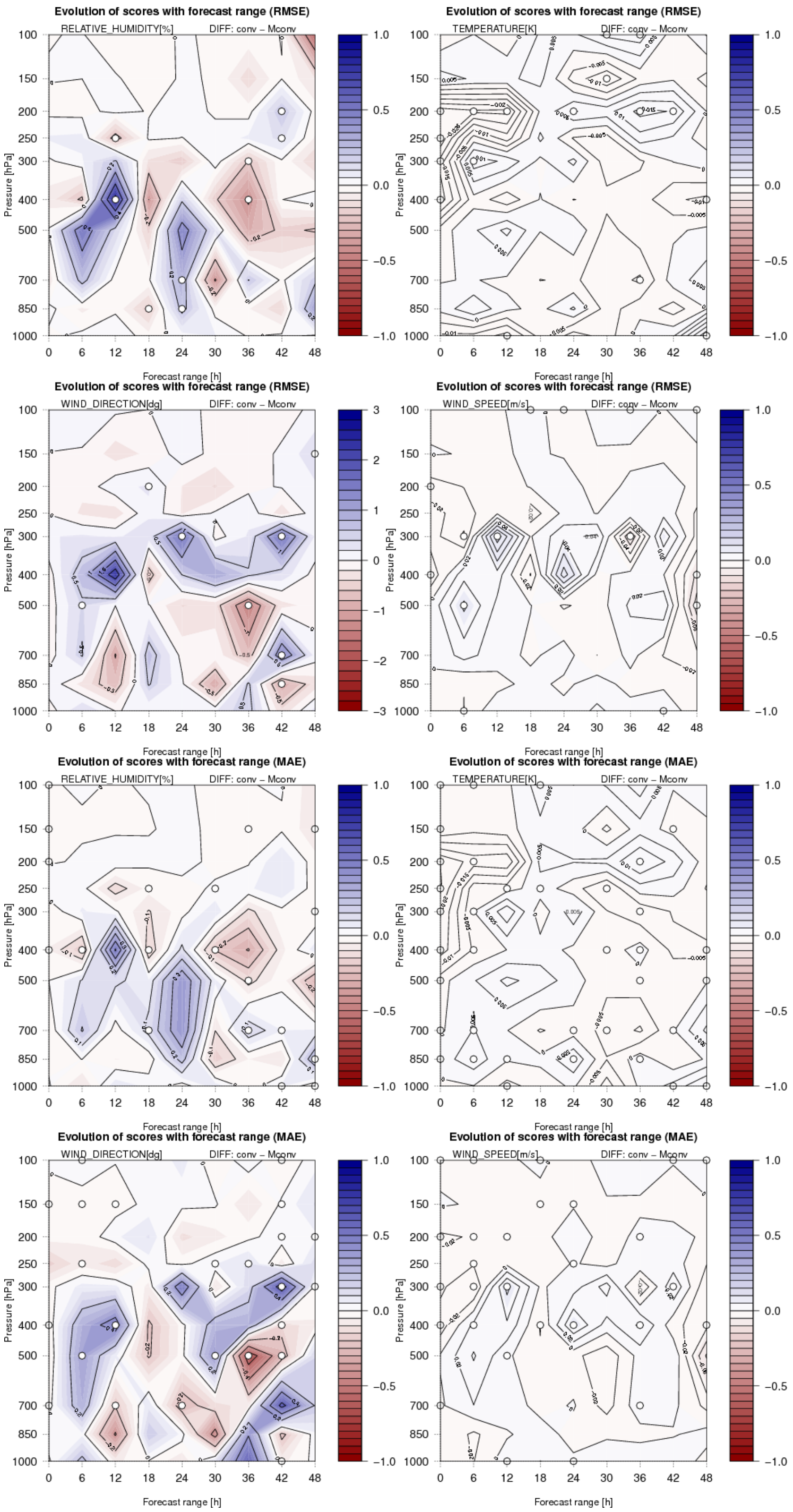

Figure 11: The forecast impact of MRAR data assimilation for the tuned 3D-VAR assimilation system. The RMSE (top) and MAE (bottom) scores are evaluated with regards to TEMP observation. The improvement/degradation is represented by blue/red color. The white points represents 95% significance level.

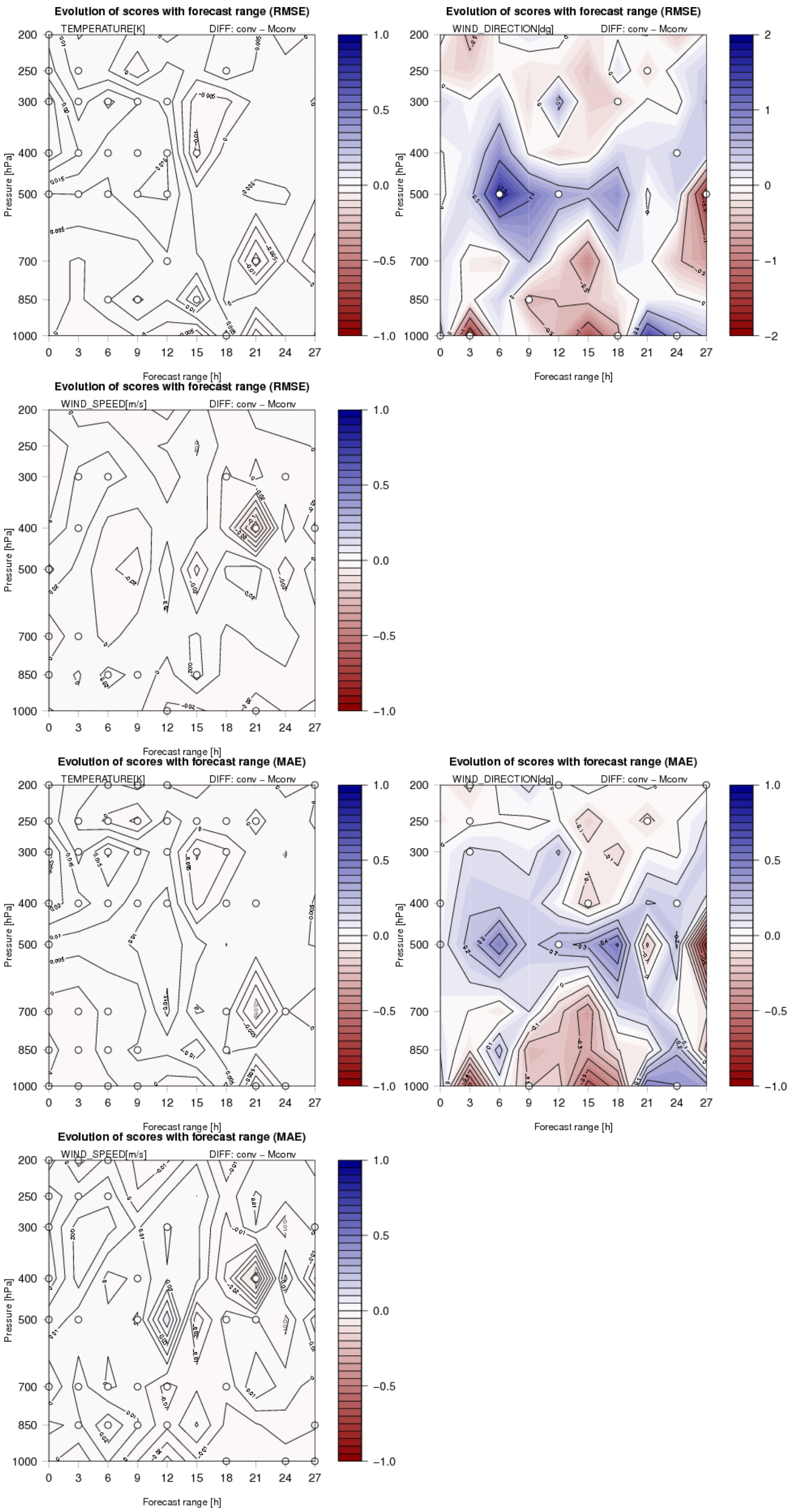

Figure 12: The forecast impact of MRAR data assimilation for the tuned 3D-VAR assimilation system. The RMSE (top) and MAE (bottom) scores are evaluated with regards to AMDAR observation. The improvement/degradation is represented by blue/red color. The white points represents 95% significance level.

6 Conclusion

In the current operational assimilation systems at the CHMI, all observation error correlations are assumed to be zero. This is a reasonable assumption for pairs of observations measured by distinct instruments, however, this assumption is entirely inaccurate for the observations that are available at higher spatial coverage than the model resolution. The aircraft Mode-S MRAR observations have been studied in detail in Aladin-CZ since 2015 [7]. According to this study, the forecast impact of MRAR data have been assessed as almost neutral (against AMDAR and TEMP), slightly positive in lower troposphere with regards to MRAR data. The aim of this study was to propose new changes in 3D-Var assimilation scheme that provide better treatment of aircrafts data in Aladin-CZ. We propose new changes in data thinning and observation error inflation for AMDAR/MRAR data that are often used in conjunction with the assumption of zero error correlations [8], [9].

In Sec 3, we studied horizontal and vertical observation error correlations of MRAR data to find an optimal thinning distance. These spatial error correlations are diagnosed by Desroziers method [11]. The error correlations are examined as a function of separation distance for the selected pressure levels in Fig 2 and Fig 3, respectively. The optimal horizontal and vertical thinning distance is estimated with regards to the threshold error correlation value of around 0.2 that was proposed by [10] for temperature parameter. Following this guidance we suggested the optimal thinning distance between $25 - 35$ km in horizontal and $15 - 20$ hPa in vertical. As a result, we use about 11% of the MRAR data that are available at each analysis time over the extended CZ domain. The forecast impact of 25-km horizontal and 18-hPa vertical thinning is shown in Fig 5 and Fig 6, respectively. The 25-km horizontal thinning improved significantly the 3-6 h forecast of the temperature and wind speed profiles (see Fig 5). Applying vertical thinning has significant positive impact on the 3-h forecast of the wind speed and wind direction vertical profiles (see Fig 6) and the impact was also detected for the 6-h forecast of the temperature and wind speed around 700 hPa (Fig 7).

In Sec 4, the observation error inflation is studied for AMDAR and MRAR data. The observation error inflation determines a weighted importance of measurements in analysis and it could be handled by sigma coefficient through the screening namelist setting.

Firstly, we estimated the observation error by the Desroziers method. We found out that the error estimations are similar between the both AMDAR and MRAR data (see Fig 8) so that we supposed to keep the same observation error settings for them in the 3D-VAR Aladin-CZ.

Secondly, an optimal error inflation is examined for the AMDAR and MRAR observations with respect to the forecast quality. The error inflation was changed through sigma coefficient from 0.7 (default sigma setting in 3D-VAR Aladin-CZ) to 5 by the step 0.7. The optimal value was examined with respect to the forecast quality (see Fig 9). As a result, the optimal value of sigma coefficient for AMDAR and MRAR observations is found around 2. This value is far away from the sigma coefficient corresponding to Desroziers error estimation (~ 0.6) as well as the current setting of sigma in 3D-Var Aladin-CZ (~ 0.7). The difference could be explained by:

- the violation of the Desroziers main assumptions
- simplification the Desroziers method by one-iteration only
- sigma coefficient was not tuned with respect to background error
- simplified **B** matrix supposing homogeneous and isotropic propagation of observation increments

Applicability of the Desroziers diagnostic for estimating of observation errors is still subject of research. Better understanding of the above mentioned issues would be essential to avoid getting mis-leading results. Consequently, we decided to use the sigma coefficient 2 as the optimal error inflation supposing that the forecast impact study provides the best empirical solution for tuning assimilation system.

Finally, we examined the forecast impact study of new data thinning (25-km horizontal and 18-hPa vertical distance) and error inflation (sigma set to 2) for AMDAR and MRAR data (called as tuned system). The tuned system for AMDAR/MRAR had positive impact on wind speed ($200 - 450$ hPa) and temperature ($450 - 850$ hPa) forecast (RMSE, MAE) up to 1-2 days. The impact of MRAR data only (not AMDAR) provided positive impact on T, WS and WD forecast in upper-troposphere (250-400 hPa) up to 9-12 hours (Fig 12). We detect also positive impact of MRAR in lower-troposphere (700-850 hPa), however, this improvement was probably very local since it was not detected with regards to TEMP observation (Fig 11).

The high spatial frequency measurements such as MRAR provide high-resolution representation of the current state of the atmosphere that is needed as initial condition for the NWP models. Based on the results there are two main issues that limit the assimilation of the high-resolution data in the 3D-VAR Aladin-CZ system namely simplified observation (**R**) and background (**B**) covariance error matrix. The assumption of zero error correlations in the **R** matrix reduces the spatial data sample (through data thinning) that could be assimilated in analysis. The simplified **B** matrix supposing homogeneous and isotropic propagation of observation increments beyond the observation points could limit the weight of observations in analysis in order to keep the signal as local as possible. Under those circumstances, the MRAR observation number is reduced to such an extent that the forecast impact of MRAR on the top of AMDAR is unexpectedly slight. Investigation of a local ensemble **B** matrix as well as observation error covariance matrix **R** is desirable in terms of the high-resolution Aladin-CZ model.

References

[1] *Kalnay E., 2003* **Atmospheric modeling, data assimilation and predictability.** Cambridge university press, 2003.

[2] *Brozkova R., et al., 2003* **Atmospheric forcing by ALADIN/MFSTEP and MFSTEP oriented tunings.** Ocean Science 2.2 (2006): 113-121.

[3] *Courtier P., et al., 1998* **The ECMWF implementation of three-dimensional variational assimilation (3D-Var). I: Formulation.** Quarterly Journal of the Royal Meteorological Society 124.550 (1998): 1783-1807.

[4] *Drue C., et al., 2008* **Aircraft type-specific errors in AMDAR weather reports from commercial aircraft.** Quarterly Journal of the Royal Meteorological Society 134.630 (2008): 229-240.

[5] *Marseille G. J., et al., 2016* **Assessment and Tuning of Data Assimilation Systems Using Passive Observations.** Quarterly Journal of the Royal Meteorological Society (2016).

[6] *Laroche S, Real S., 2013 Impact of radiosonde balloon drift on numerical weather prediction and verification.* Weather and Forecasting 28.3 (2013): 772-782.

[7] *Trojakova A., et al., 2015* **Assimilation of Mode-S observations in ALADIN/CHMI.** RC-LACE web page:
`http://www.rclace.eu/File/Data_Assimilation/2015/rep_Mode_S_201512.pdf`

[8] *Dando M. L., Thorpe A. J. and Eyre J. R., 2007* **The optimal density of atmospheric sounder observations in the Met Office NWP system.** Quarterly Journal of the Royal Meteorological Society 133.629 (2007): 1933-1943.

[9] *Collard A. D., and McNally A. P., 2009* **The assimilation of infrared atmospheric sounding interferometer radiances at ECMWF.** Quarterly Journal of the Royal Meteorological Society 135.641 (2009): 1044-1058.

[10] *Liu Z.Q., and Rabier F., 2003* **The potential of high-density observations for numerical weather prediction: A study with simulated observations.** Quarterly Journal of the Royal Meteorological Society 129.594 (2003): 3013-3035.

[11] *Desroziers, G., et al.* **Diagnosis of observation, background and analysisâĂŘerror statistics in observation space.** Quarterly Journal of the Royal Meteorological Society 131.613 (2005): 3385-3396.

[12] *Bucanek A., Benacek P., Trojakova A., 2015* **Operational implementation of BlendVar scheme at CHMI.** RC-LACE web page:
`http://www.rclace.eu/File/Data_Assimilation/reports/Bucanek_BlendVar_implementation_2015.pdf`

A Spatial data thinning

Concerning the thinning of aircraft data it is important to know that one aircraft flight consists of a set of reports. The thinning of aircraft observations is performed for each flight separately. During the thinning 3D boxes are constructed around model levels. In each box the report closest to the analysis date containing the largest number of active observations is selected. The box size is set in meters via the RMFIND_AIREP variable in the NAMSCC namelist. The horizontal thinning is controlled by the screening namelist variable:

```
RFIND_AIREP=0.5675*RA/RDEGREES
```

The vertical thinning is controlled by the variables

`RAIREPTHIN, RAIREPPCENTTHIN, RAIREPTOPPRES.`

These can be set to zero by the user if no vertical thinning is required.

B Desroziers method behavior

We investigate the behavior of the Desroziers method described in Sec 1.3. Statistical approximation of the observation error can be find provided that observation and background errors are mutually uncorrelated (1). Following the results with simple 1-D model (Strajnar, 2010), we examined how observation error correlation and the number of iterations can influence the estimated observation error.

The observation error correlations are control by the data thinning distance. The sparser data are the less error-correlations appear. The dependence of the estimated observation error on data thinning is shown for MODE-S in Fig 13. Note that for observation error is significantly under-estimated for the 5-km data thinning, while using the higher thinning distance then 25-km the observation error correlation could be almost neglected. These results are in agreement with the observation error correlations separated by observation distance in Fig 2.

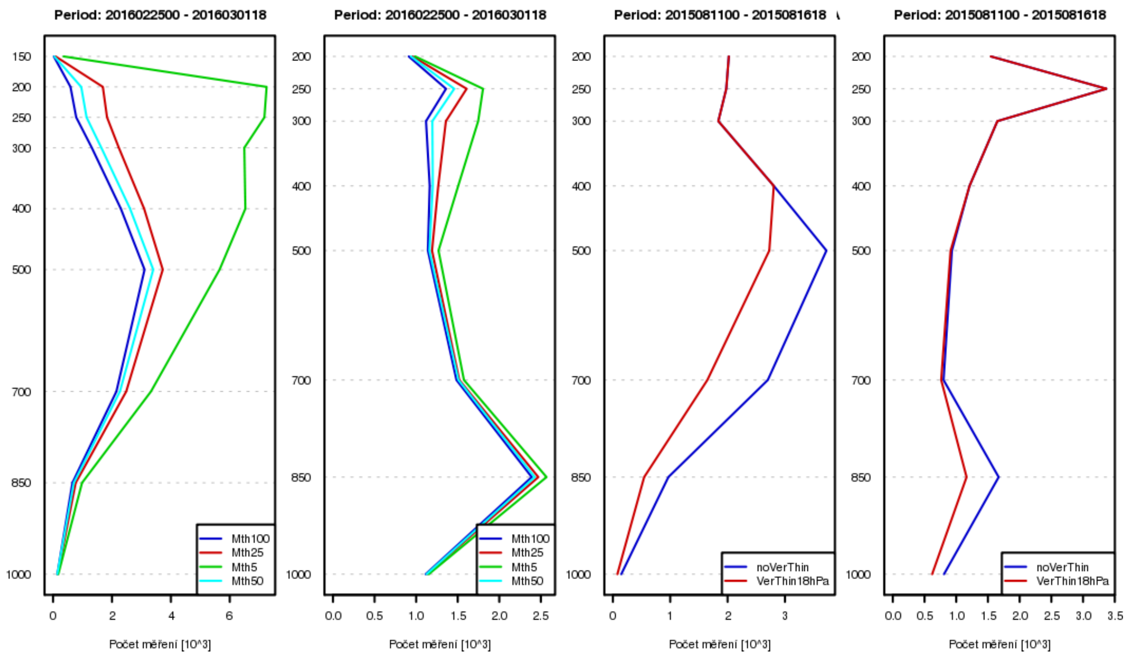

Figure 13: The behavior of Desroziers observation error estimation with regard to 5-, 25-, 50- and 100-km data thinning.

The Desroziers method is an iterative method. One should redo the analysis with new estimated observation error to obtain new estimates. However, it has been shown by Desroziers et al. (2005) that the iteration converges quickly and so the first estimate is not too far from the final converged value. Moreover, the speed of convergence increases with the number of observations (Chapnik et al., 2004). The behavior of observation errors estimation after first two iterations is shown for MODE-S (top) and

AMDAR (bottom) in Fig 14. The initial observation error is represented by the error assumed in the 3D-Var system (dashed line), while the first (red) and second (green) error-estimates are diagnosed by Desroziers method. Note that the both iterations are very close to each other comparing to the initial error-value. In addition, we include the first-error estimation diagnosed by Desroziers for the long-term 3 month period (blue) to confirm the increase of the speed of convergence. Note that the larger observation number provide more accurate first-iteration error-estimate, but this estimation is still overestimated comparing to the second-iteration estimate. Based on these results, first-iteration estimate provide a good first estimation of observation error, however, it could be still far away from the real observation error. Moreover this problem could be enhanced by the violation of the Desroziers method assumptions in (1).

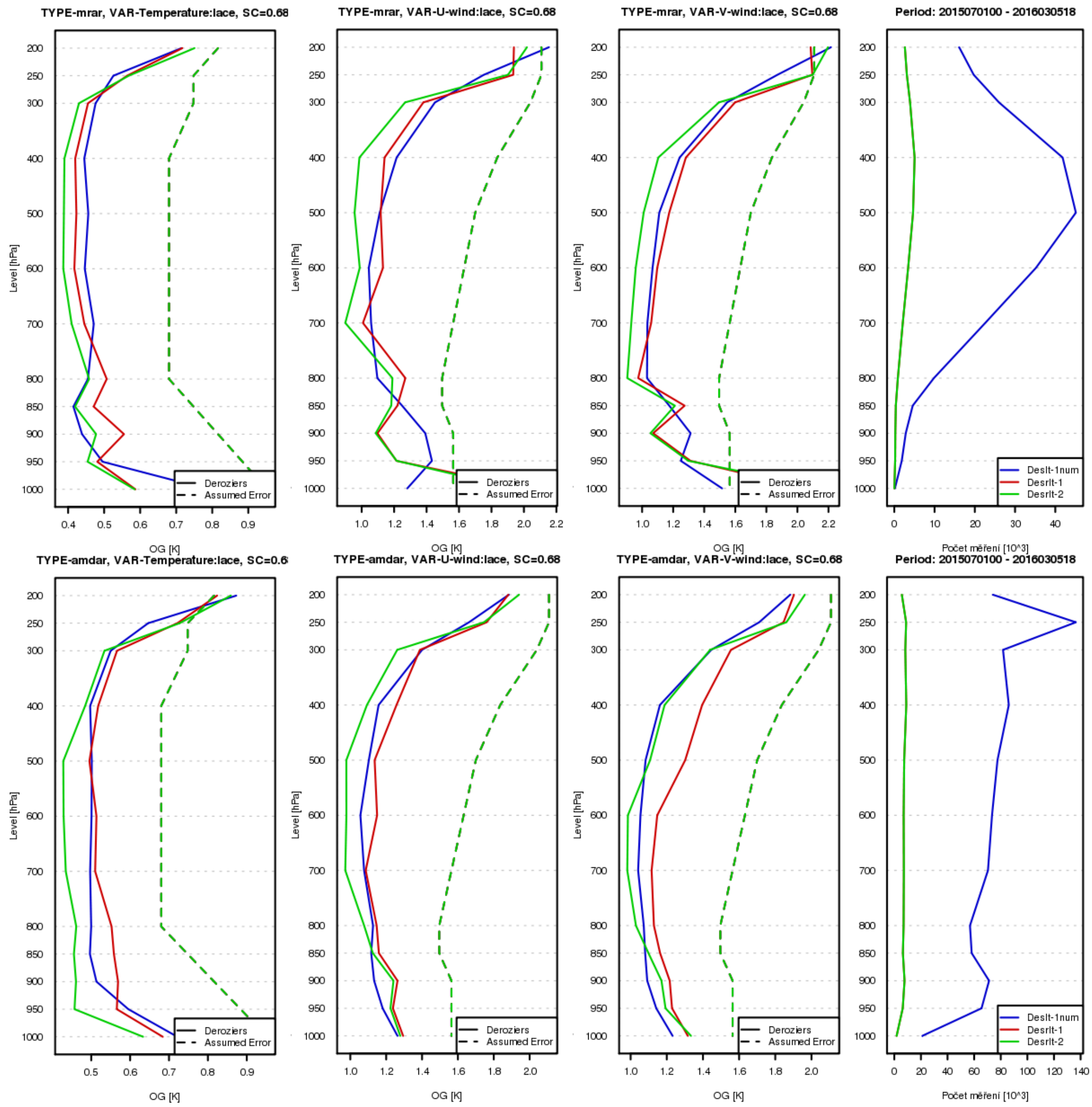

Figure 14